

Durability of self-healing cementitious systems with encapsulated polyurethane evaluated with a new pre-standard test method

*Original*

Durability of self-healing cementitious systems with encapsulated polyurethane evaluated with a new pre-standard test method / Anglani, Giovanni; Van Mullem, Tim; Tulliani, JEAN MARC CHRISTIAN; Van Tittelboom, Kim; De Belie, Nele; Antonaci, Paola. - In: MATERIALS AND STRUCTURES. - ISSN 1359-5997. - ELETTRONICO. - 55:5(2022).  
[10.1617/s11527-021-01818-3]

*Availability:*

This version is available at: 11583/2970428 since: 2022-08-03T08:56:01Z

*Publisher:*

SPRINGER

*Published*

DOI:10.1617/s11527-021-01818-3

*Terms of use:*

openAccess

This article is made available under terms and conditions as specified in the corresponding bibliographic description in the repository

*Publisher copyright*

(Article begins on next page)



# Durability of self-healing cementitious systems with encapsulated polyurethane evaluated with a new pre-standard test method

Giovanni Anglani · Tim Van Mullem · Jean-Marc Tulliani · Kim Van Tittelboom · Nele De Belie · Paola Antonaci

Received: 3 March 2021 / Accepted: 4 November 2021 / Published online: 1 June 2022  
© The Author(s) 2022

**Abstract** This work reports on the self-healing capabilities of mortar specimens with polyurethane encapsulated in two types of cementitious macro-capsules, by comparison with the performance of mortar specimens using the same healing agent encapsulated in glass capsules, as tested in an inter-laboratory testing campaign following a pre-standard procedure. This comparison was performed with a twofold objective of checking the robustness of such pre-standard procedure for varying types of capsules and testing the effectiveness of a new type of

cementitious capsule that has never been used before in durability tests. The testing procedure was developed in the framework of the EU COST Action SARCOS. First, the specimens were pre-cracked via three-point bending followed by an active crack width control technique. Then, the self-healing effect was characterised in terms of water permeability reduction. The cementitious capsules offered equivalent or better performance compared to the glass capsules used in the inter-laboratory testing. The average sealing efficiency for the specimens containing cementitious capsules ranged from 54 to 74%, while for glass macro-capsules it was equal to 56%. It was also observed that when applying the pre-standard procedure to test specimens containing capsules with comparable size and geometric arrangement, the same results were obtained in different repetitions of the test. The results obtained confirmed the possibility to use the cementitious capsules as a valid macro-encapsulation system, offering additional advantages compared to glass capsules. The repeatability of the results corroborated the robustness of the adopted testing procedure, highlighting its potential for further standardisation.

---

G. Anglani (✉) · P. Antonaci  
Department of Structural, Geotechnical and Building Engineering, Politecnico di Torino, Corso Duca degli Abruzzi 24, 10129 Torino, Italy  
e-mail: giovanni.anglani@polito.it

G. Anglani · P. Antonaci  
Responsible Risk Resilience Centre, Politecnico di Torino, Viale Mattioli 39, 10125 Torino, Italy

T. Van Mullem · K. Van Tittelboom · N. De Belie  
Magnet-Vandepitte Laboratory, Department of Structural Engineering and Building Materials, Faculty of Engineering and Architecture, Ghent University, Tech Lane Ghent Science Park, Campus A, Technologiepark Zwijnaarde 60, B-9052 Gent, Belgium

J.-M. Tulliani  
INSTM Research Unit PoliTO-LINCE Laboratory, Department of Applied Science and Technology, Politecnico di Torino, Corso Duca degli Abruzzi 24, 10129 Torino, Italy

**Keywords** Self-healing · Cementitious materials · Standardisation · Cementitious capsules · Polyurethane · Water permeability



## 1 Introduction

Self-healing materials are man-made materials, which have the built-in capability to repair structural damage autogenously due to their composition, autonomously by embedding unconventional engineered additions in their matrix, or with the minimal help of an external stimulus [1–4]. In the past decades, different types of self-healing materials were investigated for different applications, such as polymers [5–7], ceramics [8, 9], metals [10], or soft materials [11, 12]. For what concerns civil engineering applications, the two main materials that are thoroughly investigated to build-in or improve the self-healing capabilities are cementitious materials [2, 3, 13] and asphalt materials [4, 14–16]. Cement is the second most used substance in the world after water and cement-based materials make up a substantial proportion of the built environment [17]. From this consideration follows the importance of improving the durability of cementitious materials, to guarantee high safety standards to their final users and reduce the high costs connected to their maintenance and repair. Moreover, the construction sector has major impacts on the environment, which comprise the consumption of raw materials and the emission of greenhouse gas during construction, maintenance, and renovation [18]. Consequently, self-healing cementitious materials could help to reduce this environmental footprint by granting a longer service life with less maintenance interventions [19], thus allowing a higher sustainability for concrete structures and infrastructures.

Accordingly, many different self-healing techniques have been developed and investigated in the last decades, such as the stimulation of their intrinsic autogenous healing capabilities through the mechanical limitation and control of the crack width [20–23] or through the use of crystalline admixtures [24–27], mineral additives [28–30], or superabsorbent polymers [31–35]. Another promising strategy is the application of an autonomous healing mechanism via micro-encapsulation [36–41], macro-encapsulation [42–46], or vascular systems [47–51]. Many different healing agents were used, either polymeric [52–55], mineral [56–59], or bacterial [60–62].

Several test methods [63, 64] and numerical models [65] were developed and used to study the effectiveness of self-healing cementitious materials. Moreover, the advances in the research and development of self-

healing cementitious materials are supported by the progressive creation of pilot projects to test their effectiveness on-site [66–70]. However, the lack of standardised test methods for self-healing cementitious materials hinders the comparison between different studies and it hampers commercialisation since the construction sector is used to a strictly regulated concrete production [71].

To solve this issue, six different inter-laboratory testing programs have been established within the framework of the EU COST Action CA 15,202 SARCOS (Self-healing As preventive Repair of CONcrete Structures) to evaluate test methods to assess the efficiency of self-healing cementitious materials, and provide inputs for their subsequent standardisation. The results of two of the six inter-laboratory testing programs are already available in literature [71, 72] and their data are completely accessible by the scientific community [73, 74]. Among them, one was dedicated to the evaluation of test methods to assess the efficiency of pre-placed macro-capsules containing polymeric healing agent and was tested by six European universities [71], using mortar and concrete specimens. Hereafter, it will be referred to as the SARCOS protocol, for the sake of brevity.

The technological interest in developing (and subsequently in characterizing) macro-capsule based self-healing systems lies in several factors. In fact, while other encapsulated self-healing systems such as micro-capsules can be uniformly distributed in the mix, thus facilitating the casting operations, macro-capsules can be placed ad hoc at specific locations (e.g., close to the reinforcement, where cracks are expected to cause potential rebar corrosion issues). In this way, they can provide a more localized repairing effect. By creating relatively weak points in the mechanical structure, they can also increase the probability to be crossed by cracks, thus triggering the self-healing mechanism. In addition, macro-capsules can store a higher quantity of healing agents with respect to micro-capsules and consequently they can be suitable to repair larger cracks.

The macro-capsules that were used in the inter-laboratory testing program were tubular glass capsules filled with polyurethane. Glass capsules were chosen due to the extensive reports available in literature that showed positive results in using this technology for encapsulation of healing agents in cementitious



materials as a proof-of-concept [42, 44, 54, 75–77]. Nevertheless, different materials were proposed in literature as valid alternatives to glass capsules, also because of possible adverse characteristics of the latter, such as their high brittleness which could result in fracture during concrete mixing and the possibility to trigger alkali-silica reactions in the cementitious matrix [78]. These alternatives include ceramic capsules [45], polymeric capsules obtained either by extrusion [46, 78–80] or additive manufacturing [81, 82], and cementitious capsules [43, 83]. Cementitious capsules were proven effective in encapsulating different types of healing agents [84] including polyurethane healing agents similar to the one used in the inter-laboratory testing. While being less brittle than the glass ones, the cementitious capsules are still efficient for repairing small cracks that could be considered harmful for the durability of concrete structures since their crack occurrence was detected in a previous study for crack mouth opening displacements not exceeding 240  $\mu\text{m}$  during pre-cracking [85], hence for smaller crack widths at the level of the capsules. They also offered good recovery both in terms of mechanical properties [85] and durability-related properties through crack sealing [84]. Moreover, cementitious capsules present an inherent compatibility between the capsules' shell and the cementitious matrix while showing the ability to survive the concrete mixing process.

In this study, the self-healing performances offered by the use of cementitious capsules were compared with those obtained with the glass capsules used in the abovementioned inter-laboratory testing campaign [71, 73] under the same protocol. The aim of such comparison was twofold: on one hand, a first goal was to test the effectiveness of the cementitious capsules with a pre-standard method, as a function of different settings and manufacturing procedures, some of which were investigated here for the first time; on the other hand, an additional goal was to prove the SARCOS protocol robustness and applicability to different self-healing cementitious materials based on the use of macro-capsules with polymeric healing agents.

The adopted testing protocol started with pre-cracking the specimens, after the application of a carbon fibre reinforced polymer strip on top of them. Immediately after pre-cracking, the crack width was reduced to a target value using an active crack width control technique [84, 86–88] in order to reduce the

crack width variability between specimens. Finally, once the crack width was controlled, and the healing agent reaction occurred and stabilised, all the specimens were subjected to a water permeability test [63, 89, 90] to assess the sealing efficiency.

## 2 Materials

### 2.1 Cementitious capsules

Cementitious capsules were produced using a polymer-modified cement paste in accordance with the mix design used in [85] and reported in Table 1. The ingredients of the paste were:

- Portland cement (CEM I 52.5 R, Buzzi Unicem S.p.A., Italy);
- Calcium carbonate ( $\text{CaCO}_3$ , Sinopia s.a.s., Italy), which was added as a superfine aggregate to reduce the capsules porosity and avoid the collapse of the capsules immediately after production;
- Metakaolin (halloysite from Applied Minerals Inc., NY, USA, calcined at 650  $^\circ\text{C}$  for 3 h), added for its high pozzolanic activity;
- Hydroxypropyl methylcellulose (HPMC, Sigma Aldrich, Italy) which was added to control the structural breakdown and reconstruction phenomena during the moulding process and to retard the paste setting;
- Demineralised water;
- Copolymer of ethyl acrylate (EA) and methyl methacrylate (MMA) (Primal B60A, Sinopia s.a.s., Italy), which was added to reduce the water/cement ratio and improve the workability of the paste;
- Polyethylene glycol (PEG, Sigma Aldrich, Italy), which was added to reduce the paste shrinkage.

The mixing was also performed in accordance with [85], using an overhead stirrer (RW 20, IKA, Germany). After mixing, the fresh cement paste was used to produce cementitious tubes according to two different manufacturing processes: the first consisted in rolling the fresh paste around an oiled bar with a circular cross-section which was later removed, obtaining a smooth cementitious tube with a hollow circular cross-section (external diameter:  $\Phi_{\text{external}} = 8 \text{ mm}$ ; internal diameter:  $\Phi_{\text{internal}} = 5 \text{ mm}$ ) [85]. The second manufacturing process was extrusion [43, 83–85, 91], which allowed to obtain ridged tubes

**Table 1** Mix design of the polymer-modified cement paste

Components	Percentage by mass (wt%)
Cement CEM I 52.5 R	46.2
Demineralised water	12.8
Calcium carbonate	21.3
Copolymer of ethyl acrylate and methyl methacrylate	17.0
Polyethylene glycol	1.7
Hydroxypropyl methylcellulose	0.7
Metakaolin	0.3

with a hollow ovoid cross-section ( $\Phi_{\text{external}} = 10$  mm,  $\Phi_{\text{internal}} = 7.5$  mm, on average). In both cases, the cementitious tubes were left for 7 days in a moist environment ( $T \approx 20$  °C and relative humidity (RH)  $> 95\%$ ) and subsequently exposed to air ( $T \approx 20$  °C,  $\approx 60\%$  RH) for complete curing over 28 days. Afterwards, they were further cut with a saw into smaller tubes. After preparing the surfaces of the tubes by immersion in a primer (Primer AQ, API SpA, Italy), an epoxy coating (Plastigel, API SpA, Italy) was applied to the internal surface of the tubes, with a thickness of about 1 mm, which reduced the internal diameter to 3 mm for the rolled capsules and 5.5 mm for the extruded capsules. The epoxy coating was needed to guarantee an adequate waterproofing of the capsule, and hence to avoid that any moisture present in the fresh mortar mix could be transferred to the core of the capsule through the pores of its cementitious shell during the casting operations. The lengths of the cementitious capsules were set to 60 and 45 mm, respectively. These length values were chosen in such a way to contain an equal or double net volume of encapsulated healing agent with respect to the glass capsules (that measured 3 mm in the internal diameter, 3.35 mm in the external diameter and 55 mm in overall length, thus allowing to introduce  $\approx 0.3$  mL of healing agent). In fact, the effective length of the cementitious capsules was reduced due to the sealing of the ends (which was done with a two-component epoxy plaster, Stucco K, API SpA, Italy). A small amount of air was also inevitably entrapped in the capsules, so that eventually a volume of approx. 0.3 mL of healing agent was encapsulated in the rolled capsules (the same as for the glass capsules), while double of this volume was encapsulated in the extruded capsules ( $\approx 0.6$  mL).

The polymeric healing agent which was used in this work to fill the capsules was the same one-component

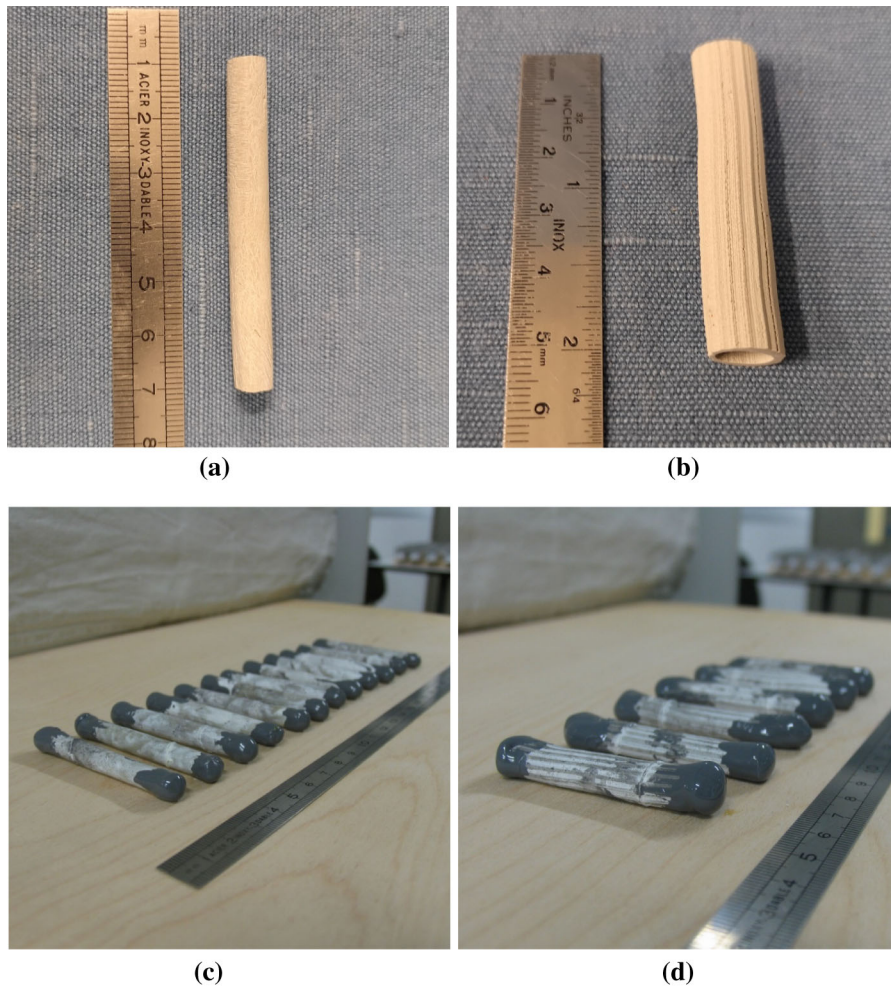
commercially available polyurethane (PU) precursor (HA Flex SLV AF, GCP Applied Technologies, Belgium) that was used in the inter-laboratory study. The precursor is characterised by a low viscosity ( $< 250$  mPa.s at 25 °C) and it polymerises upon contact with moisture. To highlight the leakage of PU, a small amount of fluorescent powder dye (EpoDye, Struers, the Netherlands) was mixed into the precursor.

Figure 1 shows the capsules after coating, filling, and sealing: on the left side of the picture, it is possible to see the capsules obtained by rolling with a small diameter (Fig. 1a, c, CEM\_S capsules), and on the right side those extruded and with a relatively larger diameter (Fig. 1b, d, CEM\_L capsules). The cementitious capsules produced by rolling were investigated here for the first time in terms of their effectiveness in allowing the recovery of durability-related properties.

The main characteristics of the cementitious capsules used in this study are summarised in Table 2.

## 2.2 Mortar specimens

Unreinforced mortar prisms ( $40 \times 40 \times 160$  mm<sup>3</sup>) were cast using a standardised mortar mix composition, as described in EN 196-1. Portland cement (CEM I 42.5 N, Buzzi Unicem S.p.A., Italy), normalised sand (grading 0–2 mm, DIN EN 196-1), and tap water were used. The water to cement ratio was 0.50, the sand to cement ratio was 3. By comparison, the mortar composition used in the inter-laboratory study was slightly different in terms of sand to cement ratio, and it was also added with a limestone filler and a superplasticiser, as reported in [71]. Concerning the mixing procedure of the mortar used in this study, cement and water were first mixed at low speed for 30 s (Hobart Mixer Model N-5, Hobart, US), after which the sand was added for the next 30 s at the same



**Fig. 1** Small-diameter capsules (CEM\_S capsules) and large-diameter capsules (CEM\_L capsules), respectively before coating (a, b) and after coating, filling, and sealing (c, d)

speed. The mixing operation continued for another minute with increased speed. The mixer was stopped and any mortar sticking to the sides of the mixing bowl was manually scraped off in 30 s, then the mixture was left to rest for one minute. Finally, the mortar was mixed for an additional minute at high speed. The casting was done in accordance with EN 196-1, hence the moulds were filled in two layers and every layer was compacted on a jolting table by 60 jolts. The moulds were covered in plastic foils until demoulding.

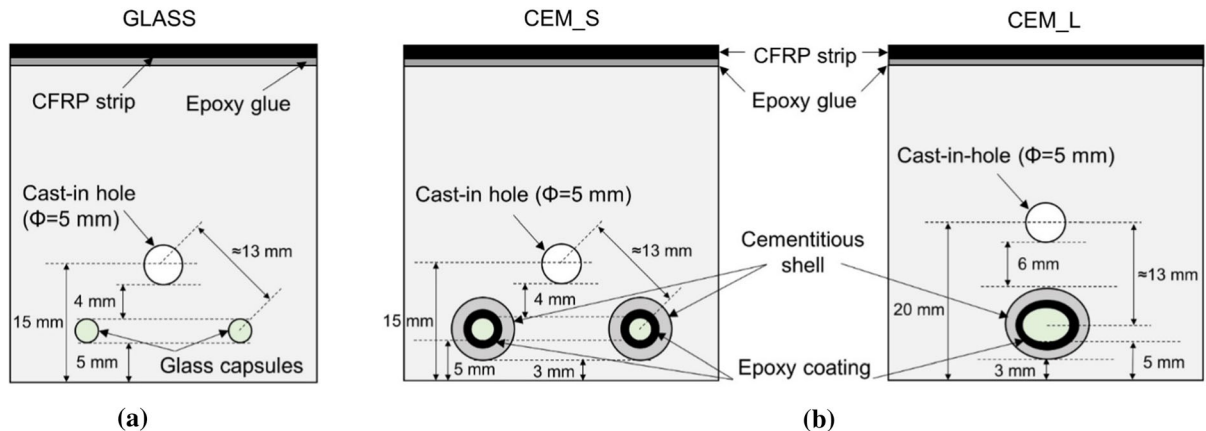
The self-healing specimens used in the inter-laboratory test [71] were also mortar prisms of the same dimensions and contained two glass capsules each, summing up to a total amount of healing agent of

$\approx 0.6$  mL. They will be hereafter referred to as GLASS series.

In a similar way as the GLASS series, two self-healing series of specimens with cementitious capsules were produced: one containing two rolled capsules (CEM\_S series, 6 specimens), one containing one extruded capsule (CEM\_L series, 6 specimens). The capsules were fixed in position by glueing them on top of two thin nylon threads previously mounted in the moulds at a height of 3 mm above the bottom side of the specimen so that, taking into account the shell and coating thicknesses, the vertical distance between the internal lower edge of the capsules and the bottom side of the specimen was approximately equal to that of the glass capsules ( $\approx 5$  mm, see Fig. 2).

**Table 2** Summary of the characteristics of capsules used for the different series

	GLASS	CEM_S	CEM_L
Manufacturing process	Extrusion	Rolling	Extrusion
Tubular shell material	Borosilicate glass	Polymer-modified cement paste	Polymer-modified cement paste
Average internal diameter of the tubular shell (mm)	3	5	7.5
Average external diameter of the tubular shell (mm)	3.35	8	10
Average length of the capsule (mm)	55	60	45
Average thickness of the epoxy coating (mm)	–	1	1
Average internal diameter after epoxy coating (mm)	–	3	5.5
Net volume of encapsulated healing agent (mL)	≈ 0.3	≈ 0.3	≈ 0.6

**Fig. 2** Self-healing mortar specimens: **a** series used in the inter-laboratory study containing glass capsules (GLASS series) [71]; **b** series used in the present study containing cementitious capsules (CEM\_S and CEM\_L series)

The specimens were provided with a cast-in hole to perform the water flow test. The longitudinal cast-in hole was obtained by placing in the mould a smooth steel bar (diameter of 5 mm) covered with demoulding oil, which was removed upon demoulding. The cast-in hole was located with its centre at 15 mm from the bottom side of the specimens in the case of the CEM\_S series, in accordance with the geometric settings and testing conditions of the inter-laboratory study. Conversely, in the case of the CEM\_L series, it was necessary to move the cast-in hole upwards to a height of 20 mm from the bottom, because of the cross-section size of the extruded capsules (see Fig. 2). This height was chosen also in order to keep the length of the segments connecting the centre of the capsules and

the centre of the cast-in hole constant in all the series (see Fig. 2). To take into account the influence of the different position of the cast-in hole, two series of reference mortar specimens without capsules were produced to be compared with their respective self-healing series: one with the lower cast-in hole (REF\_S series, 6 specimens) and one with the higher cast-in hole (REF\_L series, 6 specimens). The companion series of the GLASS series, which was tested in the inter-laboratory study, will be hereafter referred to as REF\_G series. While presenting the same configuration as the REF\_S series in terms of cast-in hole position, this series had a slightly different mortar composition, as previously mentioned. Therefore, it was decided to include it in this study in addition to the

REF\_S series for the sake of comparison with the GLASS series, which in fact was produced with the same mix composition and casting conditions as REF\_G.

After demoulding, the specimens were sealed in plastic foil in groups of 3 to maintain the same curing condition as for the series used in the inter-laboratory study.

### 3 Methods

#### 3.1 Crack creation and active crack width control

Before crack creation, a carbon fibre reinforced polymer (CFRP) strip (Sika® CarboDur®, Sika Italia, Italy) with comparable characteristics to the CFRP strips used in the inter-laboratory test and with the same dimensions ( $40 \times 160 \text{ mm}^2$ ) was glued on top of the specimens using an epoxy resin (Sikadur®-30, Sika Italia, Italy) (see Fig. 2). At an age of 7 days, the specimens were cracked in a three-point bending test with a span of 100 mm and a loading rate of 50 N/s. Since there was no tensile reinforcement in the specimens, they failed suddenly; however, both halves remained connected due to the CFRP, which allowed to widen or close the cracks arbitrarily to apply the active crack width control [86, 87]. Immediately after cracking, the specimens were placed with their crack mouth facing upwards and the crack width was restrained using screw jacks under an optical microscope using an iterative procedure of measuring and restraining until the average crack width fell within a desired crack width range of 290–310  $\mu\text{m}$ . This range was chosen because cracks presenting a width of 300  $\mu\text{m}$  are the most addressed in the studies concerning self-healing cementitious materials, in consideration of the serviceability limit state design in the Eurocodes [92, 93].

Along the crack path, three different locations were chosen to measure the crack width. The locations were not fixed, as indicated in the guidelines provided in the inter-laboratory testing [73], in order to avoid the risk of studying a location with a defect (e.g., a missing aggregate or sand particle, (semi) loose particles, missing pieces of the cementitious matrix, parallel cracks, etc.), resulting in the measurement of a local phenomenon, instead of a global description of the crack [71]. Consequently, the operator chose locations

representative of the crack, preventing overlap and striving towards a uniform distribution of the three measurement locations along the crack length. In each location, the crack width was measured 5 times. Hence, the average crack width was calculated as the average of the 15 crack width measurements.

The active crack width control was executed in less than 30 min. Finally, the specimens were turned so that the crack mouth would be facing downwards again.

#### 3.2 Water permeability

The water permeability of the cracked specimens was measured using a water flow test [63, 89, 90]. Prior to executing the test, the specimens were stored in an air-conditioned room ( $T = 20 \text{ }^\circ\text{C}$ , 60% RH) with their crack facing downwards for at least 1 day after crack creation, to allow the PU to polymerise by contact with humid air. Subsequently, the specimens were submerged in demineralised water for 24–48 h to prevent the influence of water absorption by the matrix on the water flow test results. Afterwards, the specimens were taken out of the water and were surface-dried. To allow the connection of the specimens to the water flow setup, the cast-in hole was enlarged on one side to a diameter of 6 mm over a length of  $25 \pm 5 \text{ mm}$  using a drill before cracking. A short plastic tube (length of  $\approx 60 \text{ mm}$ ,  $\Phi_{\text{external}} = 6 \text{ mm}$ ,  $\Phi_{\text{internal}} = 4 \text{ mm}$ ) was then inserted in the enlarged cast-in hole and leakages were prevented using silicone. The other side of the cast-in hole was sealed completely with silicone. The plastic tube was then connected to a tube in contact with an open water reservoir. The water head, measured from the centre of the cast-in hole up to the water level, was kept constant throughout the test at  $50 \pm 2 \text{ cm}$  by topping up with demineralised water, in order to maintain a constant pressure ( $\approx 0.05 \text{ bar}$ ). In order to measure only the water leaking out of the crack mouth, the sides of the specimens (at the location of the crack) were sealed prior to saturation by using viscous methyl methacrylate glue (Schnellklebstoff X60, HBM, Germany), allowing water to only leak out of the bottom side of the specimens, see Fig. 3a. The first 60 s of water leakage were not recorded in order to measure only a fully developed flow and to allow the removal of water bubbles from the system. Subsequently, the weight of the water which leaked from the crack was recorded for a



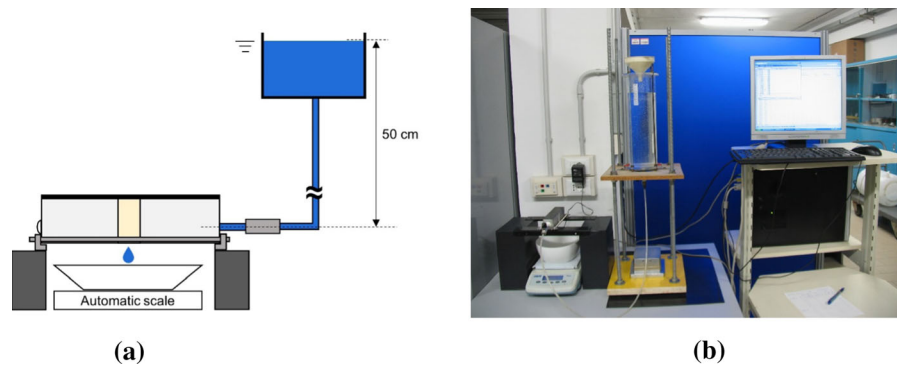


**Fig. 3** Water flow test setup: **a** graphical scheme; **b** actual setup

minimum of 6 min. Figure 3 shows the water flow test setup used to evaluate the water permeability.

The sealing efficiency  $SE_{wf}$  of each self-healing specimen was calculated with respect to the corresponding reference specimens, without capsules, using Eq. (1):

$$SE_{wf}(\%) = \frac{\bar{q}_{REF\_i} - q_j}{\bar{q}_{REF\_i}} \times 100 \quad (1)$$

where  $\bar{q}_{REF\_i}$  is the average water flow rate (g/min) of the reference specimens of each series ( $REF\_i$  could either correspond to REF\_G, REF\_S, or REF\_L) and  $q_j$  the water flow rate (g/min) of each self-healing specimen ( $j$  could either correspond to GLASS, CEM\_S, or CEM\_L).

In addition to this, in the inter-laboratory study, the spread of polyurethane on the crack surfaces of mortar specimens was quantified using segmentation techniques [32, 94, 95]. However, since it was concluded that there is no strong relationship between the surface coverage and the measured water flow [71], this analysis was not considered relevant for the present work.

## 4 Results and discussion

### 4.1 Crack creation and active crack width control

Figure 4 shows the average crack width  $\bar{w}$  ( $\mu\text{m}$ ) and the related standard deviation measured for the different series. For all the series containing cementitious capsules and their related reference companions, 6 specimens were produced and tested, with the only exception of the CEM\_S series, for which one

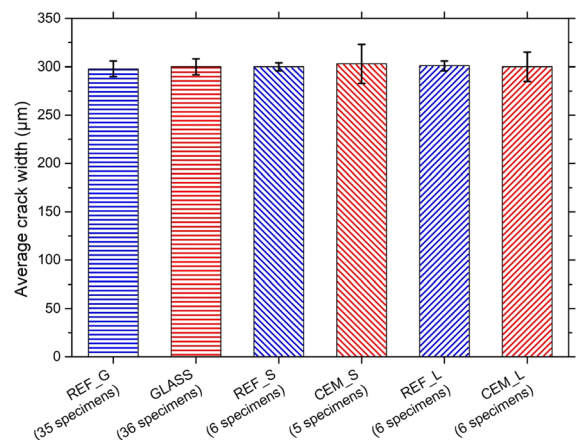


**Fig. 4** Average crack width  $\bar{w}$  of each series after the active crack width control. Error bars represent the standard deviation

specimen was accidentally broken during crack creation; therefore only 5 specimens were available for the crack width measuring and further testing of this series. The results for the REF\_G and GLASS series comprise the results obtained by each laboratory involved in the inter-laboratory testing, all grouped together respectively [71, 73]. In fact, the crack width of the specimens of all labs involved in the inter-laboratory study could be assumed to be statistically equal, with only a minor difference between two of the six laboratories (Tamhane's T2 post hoc test, level of significance = 0.05,  $p = 0.028$ ).

Overall, the application of the active crack width control technique was successful for obtaining an average crack width within the desired range of 290–310  $\mu\text{m}$ . All six series were statistically compared. Equality of variances could not be assumed based on a Levene's test (level of significance = 0.05,

$p = 0.003$ ). A one-way analysis of variance (ANOVA) with a Welch test showed no statistical difference with respect to the means of the six series (level of significance = 0.05,  $p = 0.931$ ). The difference in terms of group sizes between the series must be pointed out, anyway. A separate equality of means analysis on only the four series produced for this study (REF\_S, CEM\_S, REF\_L, and CEM\_L series) resulted in a higher  $p$ -value.

Both reference series (REF\_S and REF\_L) were characterised by a very low variability in crack width, combined with a clean appearance, with very few ramifications or loose particles (Fig. 5a, c). For the series with embedded cementitious capsules (CEM\_S and CEM\_L), the influence of the capsule stiffness caused crack toughening mechanisms such as bifurcation or deviation of the crack path (visible in Fig. 5b, d, e), resulting in a higher variability of the crack widths. It is important to highlight that the young age of the mortar matrix of the specimens (7 days) in comparison to the older capsule shells (28 days) may have played a role in the onset of such a mechanism, and that the cementitious capsules are much closer to concrete aggregates, rather than sand grains, both for their size and mechanical properties. Hence, it can be expected that they should work better when added to a concrete mix, rather than to a mortar mix.

In the case of the small-diameter cementitious capsules, the released polyurethane was not clearly visible over the crack mouth (Fig. 5b), presumably due to capillary resistive forces exerted by the capsule. It is also important to highlight the influence over the polyurethane's release mechanism exerted by the

selected crack creation method, which induced a brittle crack formation with a large crack width appearing suddenly. If cracks were slowly created, the capillary suction forces in the early-stage small cracks would have been able to overcome the capillary resistive forces in the small diameter cementitious capsules, allowing a better release of the polyurethane.

For the specimens with extruded capsules, it was possible to notice an abundant release of polyurethane, that was clearly visible over the crack mouth (Fig. 5d–f). In some cases, the amount of polyurethane leaked out from the crack mouth was such that it did not even allow to choose well-spaced locations to measure the crack width. This different release behaviour can be ascribed to the larger diameter of the capsules (i.e., a reduced capillary resistive action) and the fact that the healing agent was concentrated in a single capsule, rather than divided over two smaller capsules.

Considering the coefficient of variation (CV) of each series' crack width after the active crack width control, the highlighted variations were quite small, confirming the efficacy of the active crack width control technique. Namely, the CV was equal to 7% for CEM\_S series, 5% for CEM\_L series, and 3% or less for the other series.

#### 4.2 Water permeability

After the healing agent polymerisation and subsequent submersion in demineralised water for 1–2 days, the pre-cracked specimens were subjected to the water flow test. Figure 6 shows the flow rate  $q$  (g/min) measured for the different series. The results for the

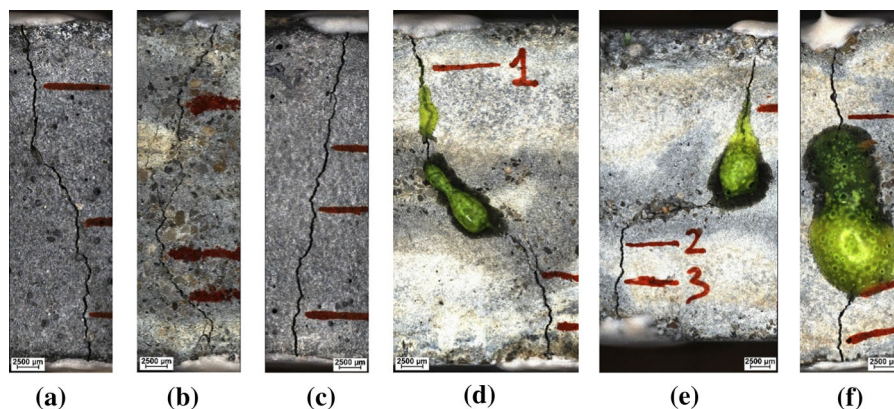


**Fig. 5** Crack mouths after the active crack width control technique: **a** REF\_S series; **b** CEM\_S series; **c** REF\_L series; **d–f** CEM\_L series. The locations used for the crack width measurements are indicated by red lines

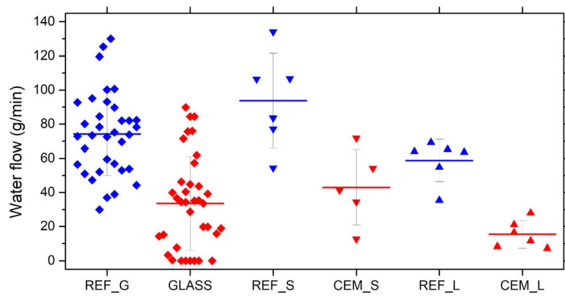


**Fig. 6** Water flow rate  $q$  of each series: individual sample results (symbols) and mean value  $\bar{q}$  of the series (solid line). Error bars represent the standard deviation

REF\_G and GLASS series comprise the results obtained by each laboratory involved in the inter-laboratory test, all grouped together respectively [71, 73], the same way as it was done for the analysis of the crack widths.

The CEM\_S and CEM\_L series obtained the same coefficients of variation for the water flow (i.e., 52%); similarly, all the reference series obtained comparable coefficients of variation (i.e., 33% for the REF\_G series, 30% for the REF\_S series, and 21% for the REF\_L series). The highest CV was calculated for the GLASS series (i.e., 82%). Comparing the coefficients of variation on the crack width (Sect. 4.1) and on the water flow, it is possible to notice that even with low variability on the crack width, the variation on the water flow is almost an order of magnitude higher, as reported in literature [86]. Indeed, Edvardsen [96] stated that the permeability of a crack is related to the third power of the crack width, hence even a small variation on the crack width will result in a higher variation on the permeability. Moreover, permeability is strongly affected by the internal geometry of the crack, on which no control can be exerted [63, 86].

A one-way ANOVA was performed for all six series after testing for equal variances (Levene's test, level of significance = 0.05,  $p = 0.122$ ). The series showed a statistically significant difference (level of significance = 0.05,  $p < 0.001$ ). It is interesting to point out that a subsequent Student–Newman–Keuls post hoc test (level of significance = 0.05) showed that all the self-healing series were statistically different from their reference series ( $p < 0.001$  for GLASS and REF\_G series,  $p = 0.005$  for CEM\_S and REF\_S series,  $p = 0.016$  for CEM\_L and REF\_L series). Also, the water flow measured for REF\_S and REF\_L

series resulted statistically different ( $p = 0.041$ ), while for REF\_S and REF\_G, which had the same cast-in hole position, no significant difference was found ( $p = 0.075$ ). Also the self-healing series did not show a significant difference ( $p = 0.162$  for CEM\_L and CEM\_S series,  $p = 0.428$  for CEM\_S and GLASS series,  $p = 0.099$  for CEM\_L and GLASS series).

When considering the self-healing specimens with two small-diameter cementitious capsules and their companion reference specimens, a steady and high flow was detected for the REF\_S series and, conversely, for the majority of the self-healing specimens of the CEM\_S series, just a constant slow dripping was visible.

Consequently, a satisfactory average sealing efficiency was assessed for the self-healing CEM\_S specimens. Namely, a reduction of 54% of the water flow with respect to the flow measured on the reference samples without capsules (REF\_S series) was calculated according to Eq. (1). A similar average sealing efficiency was obtained for the GLASS series (i.e.,  $\overline{SE}_{wf}=56\%$ ), which was tested with the same setup (i.e., with equal position of the cast-in hole and of the capsules). This similarity was also highlighted by the ANOVA analysis previously presented. These comparable results are most likely dependent on the similarities of the two self-healing systems, in terms of number of capsules, internal diameter, length, and net volume of encapsulated healing agent, resulting in similar release mechanisms and consequently sealing efficiency. Hence, it can be deduced that cementitious and glass shells are substantially equivalent from the point of view of the self-sealing effect, if the other capsule parameters are the same. In general, it can be expected that the differences in the capsule shell do not affect the release mechanism and the resulting sealing efficiency itself (for equal other settings), provided that the embedded capsules can be broken upon crack occurrence in the cementitious matrix. Therefore, the selection of the encapsulation system/capsule shell material can be made on the basis of other criteria, depending on the specific applications.

The good release of polyurethane from the specimens of the CEM\_L series containing one extruded capsule (see Fig. 5 as an example) resulted in an even lower measured water flow, which was significantly lower than in their reference counterparts (REF\_L series). Note that the mean flow rate of the REF\_L

series was lower than that of the REF\_S series, most likely due to the higher position of the cast-in hole in combination with the mode-I crack opening configuration achieved through the three-point-bending test. This configuration created a crack that can be assumed to be in the shape of an inverted V, if the tortuosity of the crack is not taken into account. Consequently, the fact that the cast-in hole was positioned higher for the REF\_L and CEM\_L series also influenced the crack width at the position of the hole. The crack width would be about 20% narrower than that at the lower cast-in hole position (REF\_S and CEM\_S series), if assuming a perfect V-shape of the crack ranging from 300  $\mu\text{m}$  at the bottom of the specimen to zero at the top, thus influencing the test results and underlining the importance of testing self-healing and reference specimens with the same cast-in hole position. The self-healing specimens of the CEM\_L series showed also a slow dripping behaviour, compared with the high flow of their reference specimens. As it might be expected, the dripping was visible just from the zone of the crack that was not covered by the PU. Consequently, a good average sealing efficiency was obtained, with a reduction of the water flow of 74% with respect to the corresponding reference specimens. This represented the best result both in comparison with the small-diameter cementitious capsules and the glass capsules, while also showing the lower variability in terms of sealing efficiency. It is interesting to point out that a similar sealing efficiency (i.e.,  $\overline{SE}_{wf} = 79\%$ ) was measured by the authors in a previous work [84] by using also in that case extruded cementitious capsules with internal coating, the same PU precursor as healing agent, and a similar testing procedure. This result further underlines the importance of repeatable and robust procedures to obtain

repeatable and comparable test results. Finally, Table 3 summarizes the results obtained for each series in terms of mean crack width, water flow and the resulting sealing efficiency.

## 5 Conclusions

In this work, the self-healing performances obtained with cementitious capsules filled with a polyurethane precursor were compared with the results from an inter-laboratory study investigating glass capsules filled with the same healing agent. The testing protocol followed in the inter-laboratory study is here referred to as SARCOS protocol.

Two series of self-healing mortar prisms were produced: one with two small-diameter capsules, the other with a single larger-diameter capsule. The first type was comparable with the glass capsules used in the inter-laboratory testing in terms of internal diameter and volume of net encapsulated healing agent, and geometric arrangement within the specimen.

The following conclusions can be drawn from the results presented in the paper:

- The application of the active crack width control technique allowed the reduction of variability in the crack width.
- The sealing efficiency was satisfactory for both series containing cementitious capsules. Reductions of 74% and 54% in the water flow rate were achieved with respect to the reference series without capsules. Concentrating the total amount of healing agent in a single capsule positively affected the final self-sealing performance.
- In general, the addition of cementitious capsules produced comparable or better performance with

**Table 3** Summary of the results for each series in terms of mean crack width and water flow, with their respective standard deviation, and the resulting sealing efficiency

	Crack width ( $\mu\text{m}$ )	Water flow (g/min)	Sealing efficiency (%)
REF_G	298 $\pm$ 8	74 $\pm$ 24	–
GLASS	300 $\pm$ 8	33 $\pm$ 27	56
REF_S	300 $\pm$ 4	94 $\pm$ 28	–
CEM_S	303 $\pm$ 20	43 $\pm$ 22	54
REF_L	301 $\pm$ 5	59 $\pm$ 12	–
CEM_L	300 $\pm$ 15	15 $\pm$ 8	74

respect to the glass capsules used in the inter-laboratory testing, for the same healing agent type and content. This result confirmed the possibility to use the cementitious capsules as a valid macro-encapsulation system, offering additional advantages such as reduced brittleness, reduced risk of alkali-silica reaction, and higher compatibility with the surrounding matrix.

- When applying the SARCOS protocol to test specimens containing macro-capsules with comparable geometric characteristics and identical arrangement within the specimens, substantially the same results are obtained in different repetitions of the test. This result contributes to validate the robustness of the SARCOS protocol for macro-capsule based self-healing systems, hence highlighting its potential for further standardisation.

**Acknowledgements** The authors would like to acknowledge networking support by the COST Action CA15202 (<http://www.sarcos.enq.cam.ac.uk>). The project has received funding from the European Union's Horizon 2020 research and innovation programme under the Marie Skłodowska-Curie grant agreement No 860006. Tim Van Mullem acknowledges the support of the grant (21SCIP-C158977-02) from the Construction Technology Research Program funded by the Ministry of Land, Infrastructure and Transport of the Korean government. The companies Tradecc, Buzzi Unicem SpA, and GCP Applied Technologies are thanked for their generous donation of materials (carbon fibre reinforced polymers, cement, and polyurethane, respectively). Beniamino Magnaghi (API SpA) is thanked for providing the waterproofing epoxy resins. The technical support of Vincenzo Di Vasto and Alberto Gallizia (Politecnico di Torino) is gratefully acknowledged.

**Funding** This work was supported by the European Cooperation in Science and Technology (SARCOS CA15202); Ministry of Land, Infrastructure and Transport of the Korean government (21SCIP-C158977-02). The project has received funding from the European Union's Horizon 2020 research and innovation programme under the Marie Skłodowska-Curie grant agreement No 860006.



## Declarations

**Conflict of interest** The authors declare that they have no conflict of interest that are relevant to the content of this article.

**Open Access** This article is licensed under a Creative Commons Attribution 4.0 International License, which permits use, sharing, adaptation, distribution and reproduction in any medium or format, as long as you give appropriate credit to the original author(s) and the source, provide a link to the Creative Commons licence, and indicate if changes were made. The images or other third party material in this article are included in the article's Creative Commons licence, unless indicated otherwise in a credit line to the material. If material is not included in the article's Creative Commons licence and your intended use is not permitted by statutory regulation or exceeds the permitted use, you will need to obtain permission directly from the copyright holder. To view a copy of this licence, visit <http://creativecommons.org/licenses/by/4.0/>.

## Appendix

Zenodo repository: <https://doi.org/10.5281/zenodo.6006671>.

## References

1. van der Zwaag S (2007) Self healing materials: an alternative approach to 20 centuries of materials science. Springer, Netherlands
2. de Rooij M, Van Tittelboom K, De Belie N, Schlangen E (2013) Self-healing phenomena in cement-based materials: state-of-the-art report of RILEM technical committee 221-SHC: self-healing phenomena in cement-based materials. Springer
3. De Belie N, Gruyaert E, Al-Tabbaa A et al (2018) A review of self-healing concrete for damage management of structures. *Adv Mater Interfaces* 5:1800074. <https://doi.org/10.1002/admi.201800074>
4. Hager MD, van der Zwaag S, Schubert US (2016) Self-healing materials. Springer International Publishing, Cham
5. Montano V, Senardi M, Van Der Zwaag S, Garcia SJ (2020) Linking interfacial work of deformation from deconvoluted macro-rheological spectrum to early stage healing in selected polyurethanes. *Phys Chem Chem Phys* 22:21750–21760. <https://doi.org/10.1039/d0cp03776a>
6. White SR, Sottos NR, Geubelle PH et al (2001) Autonomic healing of polymer composites. *Nature* 409:794–797. <https://doi.org/10.1038/35057232>
7. Blaiszik BJ, Kramer SLB, Olugebefola SC et al (2010) Self-healing polymers and composites. *Annu Rev Mater Res* 40:179–211. <https://doi.org/10.1146/annurev-matsci-070909-104532>
8. Osada T, Hara T, Mitome M et al (2020) Self-healing by design: universal kinetic model of strength recovery in self-

- healing ceramics. *Sci Technol Adv Mater*. <https://doi.org/10.1080/14686996.2020.1796468>
9. Ozaki S, Nakamura M, Osada T (2020) Finite element analysis of the fracture statistics of self-healing ceramics. *Sci Technol Adv Mater* 21:609–625. <https://doi.org/10.1080/14686996.2020.1800368>
  10. Yu H, Xu W, van der Zwaag S (2020) A first step towards computational design of W-containing self-healing ferritic creep resistant steels. *Sci Technol Adv Mater* 21:641–652. <https://doi.org/10.1080/14686996.2020.1814679>
  11. Tamate R, Watanabe M (2020) Recent progress in self-healable ion gels. *Sci Technol Adv Mater* 21:388–401. <https://doi.org/10.1080/14686996.2020.1777833>
  12. Xu H, Suzuki N, Takahashi A et al (2020) Structural reorganization and crack-healing properties of hydrogels based on dynamic diselenide linkages. *Sci Technol Adv Mater* 21:450–460. <https://doi.org/10.1080/14686996.2020.1783967>
  13. Van Tittelboom K, De Belie N (2013) Self-healing in cementitious materials—a review. *Materials* (Basel) 6:2182–2217. <https://doi.org/10.3390/ma6062182>
  14. Xu S, García A, Su J et al (2018) Self-healing asphalt review: from idea to practice. *Adv Mater Interfaces* 5:1800536. <https://doi.org/10.1002/admi.201800536>
  15. Xu S, Tabaković A, Liu X, Schlangen E (2018) Calcium alginate capsules encapsulating rejuvenator as healing system for asphalt mastic. *Constr Build Mater* 169:379–387. <https://doi.org/10.1016/j.conbuildmat.2018.01.046>
  16. Al-Mansoori T, Norambuena-Contreras J, Garcia A (2018) Effect of capsule addition and healing temperature on the self-healing potential of asphalt mixtures. *Mater Struct* 51:1–12. <https://doi.org/10.1617/s11527-018-1172-5>
  17. Scrivener KL, John VM, Gartner EM (2018) Eco-efficient cements: potential economically viable solutions for a low-CO<sub>2</sub> cement-based materials industry. *Cem Concr Res* 114:2–26. <https://doi.org/10.1016/j.cemconres.2018.03.015>
  18. Ding GKC (2014) Life cycle assessment (LCA) of sustainable building materials: an overview. In: Pacheco-Torgal F, Cabeza LF, Labrincha J et al (eds) *Eco-efficient construction and building materials: life cycle assessment (LCA)*. Woodhead Publishing, Eco-Labeling and Case Studies, pp 38–62
  19. van Breugel K (2007) Is there a market for self-healing cement-based materials? In: Schmets AJM, van der Zwaag S (eds) *Proceedings of the first international conference on self healing materials*. Springer, Noordwijk aan Zee, the Netherlands, pp 1–9
  20. Nishiwaki T, Sasaki H, Kwon S-M (2015) Experimental study on self-healing effect of FRCC with PVA fibers and additives. *J Ceram Process Res* 16:89–94
  21. Homma D, Mihashi H, Nishiwaki T (2009) Self-healing capability of fibre reinforced cementitious composites. *J Adv Concr Technol* 7:217–228
  22. Maddalena R, Bonanno L, Balzano B et al (2020) A crack closure system for cementitious composite materials using knotted shape memory polymer (k-SMP) fibres. *Cem Concr Compos* 114:103757. <https://doi.org/10.1016/j.cemconcomp.2020.103757>
  23. Jefferson A, Joseph C, Lark R et al (2010) A new system for crack closure of cementitious materials using shrinkable polymers. *Cem Concr Res* 40:795–801. <https://doi.org/10.1016/j.cemconres.2010.01.004>
  24. Ferrara L, Cuenca E, Tejedor A, Brac EG (2018) Performance of concrete with and without crystalline admixtures under repeated cracking/healing cycles. *MATEC Web Conf* 199:02016. <https://doi.org/10.1051/MATECCONF/201819902016>
  25. Roig-Flores M, Moscato S, Serna P, Ferrara L (2015) Self-healing capability of concrete with crystalline admixtures in different environments. *Constr Build Mater* 86:1–11. <https://doi.org/10.1016/j.conbuildmat.2015.03.091>
  26. Roig-Flores M, Pirritano F, Serna P, Ferrara L (2016) Effect of crystalline admixtures on the self-healing capability of early-age concrete studied by means of permeability and crack closing tests. *Constr Build Mater* 114:447–457. <https://doi.org/10.1016/j.conbuildmat.2016.03.196>
  27. De Nardi C, Bullo S, Ferrara L et al (2017) Effectiveness of crystalline admixtures and lime/cement coated granules in engineered self-healing capacity of lime mortars. *Mater Struct* 50:1–12. <https://doi.org/10.1617/s11527-017-1053-3>
  28. Alghamri R, Kanellopoulos A, Litina C, Al-Tabbaa A (2018) Preparation and polymeric encapsulation of powder mineral pellets for self-healing cement based materials. *Constr Build Mater* 186:247–262. <https://doi.org/10.1016/J.CONBUILDMAT.2018.07.128>
  29. Qureshi TS, Al-Tabbaa A (2016) Self-healing of drying shrinkage cracks in cement-based materials incorporating reactive MgO. *Smart Mater Struct* 25:084004. <https://doi.org/10.1088/0964-1726/25/8/084004>
  30. Gruyaert E, Van TK, Rahier H, De BN (2015) Activation of pozzolanic and latent-hydraulic reactions by alkalis in order to repair concrete cracks. *J Mater Civ Eng* 27:04014208. [https://doi.org/10.1061/\(ASCE\)MT.1943-5533.0001162](https://doi.org/10.1061/(ASCE)MT.1943-5533.0001162)
  31. Snoeck D, Van Tittelboom K, Steuperaert S et al (2014) Self-healing cementitious materials by the combination of microfibrils and superabsorbent polymers. *J Intell Mater Syst Struct* 25:13–24. <https://doi.org/10.1177/1045389X12438623>
  32. Romero Rodríguez C, Chaves Figueiredo S, Deprez M et al (2019) Numerical investigation of crack self-sealing in cement-based composites with superabsorbent polymers. *Cem Concr Compos* 104:103395. <https://doi.org/10.1016/j.cemconcomp.2019.103395>
  33. Mignon A, Vermeulen J, Snoeck D et al (2017) Mechanical and self-healing properties of cementitious materials with pH-responsive semi-synthetic superabsorbent polymers. *Mater Struct* 50:1–12. <https://doi.org/10.1617/s11527-017-1109-4>
  34. Snoeck D (2018) Superabsorbent polymers to seal and heal cracks in cementitious materials. *RILEM Tech Lett* 3:32–38. <https://doi.org/10.21809/rilemtechlett.2018.64>
  35. Yang H, Liu J, Zhou Q, Ji H (2019) The re-swelling behavior of superabsorbent polymers (SAPs) in hardened cement paste with an artificial crack. *Mater Struct* 52:1–13. <https://doi.org/10.1617/s11527-019-1394-1>
  36. Gilford J, Hassan MM, Rupnow T et al (2014) Dicyclopentadiene and sodium silicate microencapsulation for self-healing of concrete. *J Mater Civ Eng* 26:886–896. [https://doi.org/10.1061/\(ASCE\)MT.1943-5533.0000892](https://doi.org/10.1061/(ASCE)MT.1943-5533.0000892)
  37. Wang JY, Soens H, Verstraete W, De Belie N (2014) Self-healing concrete by use of microencapsulated bacterial

- spores. *Cem Concr Res* 56:139–152. <https://doi.org/10.1016/J.CEMCONRES.2013.11.009>
38. Souza L, Al-Tabbaa A (2018) Microfluidic fabrication of microcapsules tailored for self-healing in cementitious materials. *Constr Build Mater* 184:713–722. <https://doi.org/10.1016/J.CONBUILDMAT.2018.07.005>
  39. Guerrero A, Calvo JLG, Carballosa P et al (2015) An innovative self-healing system in ultra-high strength concrete under Freeze-Thaw cycles. In: *Nanotechnology in construction*. Springer International Publishing, pp 357–362
  40. Kanellopoulos A, Giannaros P, Al-Tabbaa A (2016) The effect of varying volume fraction of microcapsules on fresh, mechanical and self-healing properties of mortars. *Constr Build Mater* 122:577–593. <https://doi.org/10.1016/j.conbuildmat.2016.06.119>
  41. Mao W, Litina C, Al-Tabbaa A (2020) Development and application of novel sodium silicate microcapsule-based self-healing oil well cement. *Materials (Basel)* 13:456. <https://doi.org/10.3390/ma13020456>
  42. Qureshi TS, Kanellopoulos A, Al-Tabbaa A (2016) Encapsulation of expansive powder minerals within a concentric glass capsule system for self-healing concrete. *Constr Build Mater* 121:629–643. <https://doi.org/10.1016/J.CONBUILDMAT.2016.06.030>
  43. Formia A, Terranova S, Antonaci P et al (2015) Setup of extruded cementitious hollow tubes as containing/releasing devices in self-healing systems. *Materials (Basel)* 8:1897–1923. <https://doi.org/10.3390/ma8041897>
  44. Kanellopoulos A, Qureshi TS, Al-Tabbaa A (2015) Glass encapsulated minerals for self-healing in cement based composites. *Constr Build Mater* 98:780–791. <https://doi.org/10.1016/J.CONBUILDMAT.2015.08.127>
  45. Van Tittelboom K, De Belie N, Van Loo D, Jacobs P (2011) Self-healing efficiency of cementitious materials containing tubular capsules filled with healing agent. *Cem Concr Compos* 33:497–505. <https://doi.org/10.1016/j.cemconcomp.2011.01.004>
  46. Hilloulin B, Van Tittelboom K, Gruyaert E et al (2015) Design of polymeric capsules for self-healing concrete. *Cem Concr Compos* 55:298–307. <https://doi.org/10.1016/J.CEMCONCOMP.2014.09.022>
  47. Selvarajoo T, Davies RE, Gardner DR et al (2020) Characterisation of a vascular self-healing cementitious material system: flow and curing properties. *Constr Build Mater* 245:118332. <https://doi.org/10.1016/j.conbuildmat.2020.118332>
  48. Selvarajoo T, Davies RE, Freeman BL, Jefferson AD (2020) Mechanical response of a vascular self-healing cementitious material system under varying loading conditions. *Constr Build Mater* 254:119245. <https://doi.org/10.1016/j.conbuildmat.2020.119245>
  49. Mihashi H, Kaneko Y, Nishiwaki T, Otsuka K (2000) Fundamental study on development of intelligent concrete characterized by self-healing capability for strength. *Concr Res Technol* 11:21–28. [https://doi.org/10.3151/crt1990.11.2\\_21](https://doi.org/10.3151/crt1990.11.2_21)
  50. Nishiwaki T, Mihashi H, Jang B-K, Miura K (2006) Development of self-healing system for concrete with selective heating around crack. *J Adv Concr Technol* 4:267–275. <https://doi.org/10.3151/jact.4.267>
  51. Li Z, de Souza LR, Litina C et al (2020) A novel biomimetic design of a 3D vascular structure for self-healing in cementitious materials using Murray's law. *Mater Des* 190:108572. <https://doi.org/10.1016/j.matdes.2020.108572>
  52. Araújo M, Van Vlierberghe S, Feiteira J et al (2016) Cross-linkable polyethers as healing/sealing agents for self-healing of cementitious materials. *Mater Des* 98:215–222. <https://doi.org/10.1016/j.matdes.2016.03.005>
  53. Van Belleghem B, Van den Heede P, Van Tittelboom K, De Belie N (2016) Quantification of the service life extension and environmental benefit of chloride exposed self-healing concrete. *Materials (Basel)* 10:5. <https://doi.org/10.3390/ma10010005>
  54. Van Belleghem B, Van Tittelboom K, De Belie N (2018) Efficiency of self-healing cementitious materials with encapsulated polyurethane to reduce water ingress through cracks. *Mater Constr* 68:e159. <https://doi.org/10.3989/mc.2018.05917>
  55. van den Heede P, van Belleghem B, Araújo MA et al (2018) Screening of different encapsulated polymer-based healing agents for chloride exposed self-healing concrete using chloride migration tests. *Key Eng Mater* 761:152–158
  56. Alghamri R, Kanellopoulos A, Al-Tabbaa A (2016) Impregnation and encapsulation of lightweight aggregates for self-healing concrete. *Constr Build Mater* 124:910–921. <https://doi.org/10.1016/J.CONBUILDMAT.2016.07.143>
  57. Ait Ouarabi M, Antonaci P, Boubenider F et al (2017) Ultrasonic monitoring of the interaction between cement matrix and alkaline silicate solution in self-healing systems. *Materials (Basel)* 10:46. <https://doi.org/10.3390/ma10010046>
  58. Anglani G, Antonaci P, Gliozzi AS, Scalerandi M (2017) Ultrasonic investigation on the fracture-healing mechanism due to alkaline silicate solutions. In: Gdoutos EE (ed) 14th international conference on fracture (ICF14). Rhodes, Greece, pp 120–121
  59. Gliozzi AS, Scalerandi M, Anglani G et al (2018) Correlation of elastic and mechanical properties of consolidated granular media during microstructure evolution induced by damage and repair. *Phys Rev Mater* 2:013601. <https://doi.org/10.1103/PhysRevMaterials.2.013601>
  60. Wang J, Ersan YC, Boon N, De Belie N (2016) Application of microorganisms in concrete: a promising sustainable strategy to improve concrete durability. *Appl Microbiol Biotechnol* 100:2993–3007. <https://doi.org/10.1007/s00253-016-7370-6>
  61. Bundur ZB, Kirisits MJ, Ferron RD (2017) Use of pre-wetted lightweight fine expanded shale aggregates as internal nutrient reservoirs for microorganisms in bio-mineralized mortar. *Cem Concr Compos* 84:167–174. <https://doi.org/10.1016/j.cemconcomp.2017.09.003>
  62. Romero Rodríguez C, de Mendonça F, Filho F, Mercuri L et al (2020) Chemo-physico-mechanical properties of the interface zone between bacterial PLA self-healing capsules and cement paste. *Cem Concr Res* 138:106228. <https://doi.org/10.1016/j.cemconres.2020.106228>
  63. Ferrara L, Van Mullem T, Alonso MC et al (2018) Experimental characterization of the self-healing capacity of cement based materials and its effects on the material performance: a state of the art report by COST Action



- SARCOS WG2. *Constr Build Mater* 167:115–142. <https://doi.org/10.1016/J.CONBUILDMAT.2018.01.143>
64. Snoeck D, Malm F, Cnudde V et al (2018) Validation of self-healing properties of construction materials through nondestructive and minimal invasive testing. *Adv Mater Interfaces* 5:1800179. <https://doi.org/10.1002/admi.201800179>
65. Jefferson T, Javierre E, Freeman B et al (2018) Research progress on numerical models for self-healing cementitious materials. *Adv Mater Interfaces* 5:1701378. <https://doi.org/10.1002/admi.201701378>
66. Davies R, Teall O, Pilegis M et al (2018) Large scale application of self-healing concrete: design, construction, and testing. *Front Mater* 5:51. <https://doi.org/10.3389/fmats.2018.00051>
67. Van Mullem T, Gruyaert E, Caspeepe R, De Belie N (2020) First large scale application with self-healing concrete in Belgium: analysis of the laboratory control tests. *Materials (Basel)* 13:997. <https://doi.org/10.3390/ma13040997>
68. Mors R, Jonkers HM (2020) Bacteria-based self-healing concrete: evaluation of full scale demonstrator projects. *RILEM Tech Lett* 4:138–144. <https://doi.org/10.21809/rilemtechlett.2019.93>
69. Ferrara L, Bamonte P, Suesta C et al (2019) An overview on H2020 project ReSHEALience. In: *Proceedings of the IABSE symposium 2019 “towards a resilient built environment—risk and asset management”*. Guimarães, Portugal, pp 174–181
70. Al-Obaidi S, Bamonte P, Luchini M et al (2020) Durability-based design of structures made with ultra-high-performance/ultra-high-durability concrete in extremely aggressive scenarios: application to a geothermal water basin case study. *Infrastructures* 5:102. <https://doi.org/10.3390/infrastructures5110102>
71. Van Mullem T, Anglani G, Dudek M et al (2020) Addressing the need for standardization of test methods for self-healing concrete: an inter-laboratory study on concrete with macrocapsules. *Sci Technol Adv Mater* 21:661–682. <https://doi.org/10.1080/14686996.2020.1814117>
72. Litina C, Bumanis G, Anglani G et al (2021) Evaluation of methodologies for assessing self-healing performance of concrete with mineral expansive agents: an interlaboratory study. *Materials (Basel)* 14:2024. <https://doi.org/10.3390/ma14082024>
73. Van Mullem T, Anglani G, Dudek M et al (2020) Raw data and supplementary material of the fifth inter-laboratory testing program (RRT5, self-healing concrete with macrocapsules) of the EU COST action SARCOS
74. Litina C, Bumanis G, Anglani G et al (2021) Raw data and supplementary material of the second inter-laboratory testing program (RRT2, self-healing concrete with MgO-based expansive minerals) of the EU COST action SARCOS. <https://doi.org/10.5281/ZENODO.4559868>
75. Dry C (1994) Matrix cracking repair and filling using active and passive modes for smart timed release of chemicals from fibers into cement matrices. *Smart Mater Struct* 3:118–123. <https://doi.org/10.1088/0964-1726/3/2/006>
76. Dry C, McMillan W (1996) Three-part methylmethacrylate adhesive system as an internal delivery system for smart responsive concrete. *Smart Mater Struct* 5:297–300. <https://doi.org/10.1088/0964-1726/5/3/007>
77. Van Tittelboom K, Snoeck D, Vontobel P et al (2013) Use of neutron radiography and tomography to visualize the autonomous crack sealing efficiency in cementitious materials. *Mater Struct* 46:105–121. <https://doi.org/10.1617/s11527-012-9887-1>
78. Araújo M, Chatrabhuti S, Gurdebeke S et al (2018) Poly(methyl methacrylate) capsules as an alternative to the proof-of-concept’ glass capsules used in self-healing concrete. *Cem Concr Compos* 89:260–271. <https://doi.org/10.1016/J.CEMCONCOMP.2018.02.015>
79. Šavija B, Feiteira J, Araújo M et al (2016) Simulation-aided design of tubular polymeric capsules for self-healing concrete. *Materials (Basel)* 10:10. <https://doi.org/10.3390/ma10010010>
80. Gruyaert E, Van Tittelboom K, Sudaet J et al (2016) Capsules with evolving brittleness to resist the preparation of self-healing concrete. *Mater Constr* 66:e092. <https://doi.org/10.3989/mc.2016.07115>
81. Anglani G, Antonaci P, Carillo Gonzales SI et al (2019) 3D printed capsules for self-healing concrete applications. In: Pijaudier-Cabot G, Grassl P, La Borderie C (eds) *10th international conference on fracture mechanics of concrete and concrete structures (FraMCoS-X)*. Bayonne, France
82. De Nardi C, Gardner D, Jefferson AD (2020) Development of 3D printed networks in self-healing concrete. *Materials (Basel)* 13:1328. <https://doi.org/10.3390/ma13061328>
83. Formia A, Irico S, Bertola F et al (2016) Experimental analysis of self-healing cement-based materials incorporating extruded cementitious hollow tubes. *J Intell Mater Syst Struct*. <https://doi.org/10.1177/1045389X16635847>
84. Anglani G, Van Mullem T, Zhu X et al (2020) Sealing efficiency of cement-based materials containing extruded cementitious capsules. *Constr Build Mater* 251:119039. <https://doi.org/10.1016/j.conbuildmat.2020.119039>
85. Anglani G, Tulliani J-M, Antonaci P (2020) Behaviour of pre-cracked self-healing cementitious materials under static and cyclic loading. *Materials (Basel)* 13:1149. <https://doi.org/10.3390/MA13051149>
86. Van Mullem T, Van Tittelboom K, Gruyaert E et al (2018) Development of an improved cracking method to reduce the variability in testing the healing efficiency of self-healing mortar containing encapsulated polymers. *MATEC Web Conf* 199:02017. <https://doi.org/10.1051/mateconf/201819902017>
87. Van Mullem T, Gruyaert E, Debbaut B et al (2019) Novel active crack width control technique to reduce the variation on water permeability results for self-healing concrete. *Constr Build Mater* 203:541–551. <https://doi.org/10.1016/j.conbuildmat.2019.01.105>
88. Lefever G, Snoeck D, Aggelis DG et al (2020) Evaluation of the self-healing ability of mortar mixtures containing superabsorbent polymers and nanosilica. *Materials (Basel)* 13:380. <https://doi.org/10.3390/ma13020380>
89. Tziviloglou E, Wiktor V, Jonkers HM, Schlangen E (2016) Bacteria-based self-healing concrete to increase liquid tightness of cracks. *Constr Build Mater* 122:118–125. <https://doi.org/10.1016/j.conbuildmat.2016.06.080>
90. Gruyaert E, Debbaut B, Snoeck D et al (2016) Self-healing mortar with pH-sensitive superabsorbent polymers: testing of the sealing efficiency by water flow tests. *Smart Mater*





- Struct 25:084007. <https://doi.org/10.1088/0964-1726/25/8/084007>
91. Anglani G, Antonaci P, Tulliani J-M et al (2018) Self-healing efficiency of cement-based materials containing extruded cementitious hollow tubes filled with bacterial healing agent. In: Bertron A, Jonkers H (eds) Final conference of RILEM TC 253-MCI: microorganisms-cementitious materials interactions. RILEM Publications S.A.R.L., Toulouse, France, pp 425–431
92. Minnebo P, Thierens G, De Valck G et al (2017) A novel design of autonomously healed concrete: towards a vascular healing network. *Materials* (Basel) 10:49. <https://doi.org/10.3390/ma10010049>
93. Tsangouri E, Karaiskos G, Deraemaeker A et al (2016) Assessment of acoustic emission localization accuracy on damaged and healed concrete. *Constr Build Mater* 129:163–171. <https://doi.org/10.1016/J.CONBUILDMAT.2016.10.104>
94. Arganda-Carreras I, Kaynig V, Schindelin J et al (2016) Trainable weka segmentation: a machine learning tool for microscopy image segmentation. *Bioinformatics* 33:2424–2426. <https://doi.org/10.1111/exd.12463>
95. Romero Rodríguez C, de Mendonça F, Filho F, Chaves Figueiredo S et al (2020) Fundamental investigation on the frost resistance of mortar with microencapsulated phase change materials. *Cem Concr Compos* 113:103705. <https://doi.org/10.1016/j.cemconcomp.2020.103705>
96. Edvardsen C (1999) Water permeability and autogenous healing of cracks in concrete. *ACI Mater J* 96:448–454. <https://doi.org/10.14359/645>

**Publisher's Note** Springer Nature remains neutral with regard to jurisdictional claims in published maps and institutional affiliations.

